The mixed ullage density is also used in evaluating y. Substituting Eq. (5) into Eq. (4) and integrating from x_1 to x_2 gives

$$\Delta(u^2)_b \Big|_{x_1}^{x_2} = 2a\left[\left(1 - \frac{T_m}{Z_u T_u}\right)(x_2 - x_1) - \frac{(T_0 - T_m)}{Z_u T_u} 15.9y \ln\left(\frac{x_2}{x_1}\right)\right] \quad (6)$$

The velocity-squared decrement due to jet mixing is given directly by Eq. (1)

$$\Delta(u^2)_m \Big|_{x_1}^{x_2} = (u_0 19.2y)^2(x_2^{-2} - x_1^{-2}) \quad (7)$$

The total change is the sum

$$\Delta(u^2) \Big|_{x_1}^{x_2} = \Delta(u^2)_b \Big|_{x_1}^{x_2} + \Delta(u^2)_m \Big|_{x_1}^{x_2} \quad (8)$$

The second term is zero in the velocity core region at the jet exit.

Using this jet penetration analysis in the computer program, the mixed ullage depths were calculated for the NASA-Lewis 1-in. straight-pipe injector tests.[6] Increasing the constants in Eqs. (1) and (2) by 20% to give values of 23.0 and 19.1, respectively, improves agreement with the experimental data. The results are shown in Fig. 3a. The pressurant mass calculated as a function of expulsion time for three straight-pipe injectors is compared in Fig. 3b with the experimental data. The calculated mass of pressurant and the relative influence of the injector diameter both agree quite well with the test results. The deviations are probably influenced by interface heat and mass transfer.

Discussion

The examples in Fig. 1 also illustrate a comparison between the "distributed system" and "lumped system" approach to pressurization analysis. The distributed system includes a spatial distribution of the system variables, along the vertical tank axis in the one-dimensional model; the lumped system uses only average values of the ullage and tank wall temperatures. The lumped model is attractive for its simplicity but the examples show that it can give grossly inaccurate results for a cryogenic propellant with a thermally stratified ullage. Only the one-dimensional analysis should be used for cryogenic applications; however, the lumped model may be suitable for storable propellant applications. The examples also show the importance of using variable gas and wall properties rather than constant average values.

Conclusions

The present analytical investigation and a study of the referenced experimental data has resulted in the following conclusions:

1) Ullage mixing has a significant effect on tank pressurization performance, resulting in a reduction in gas-wall heat loss and pressurant mass requirement. The performance difference is greatest for small tanks, low tank pressures, cryogenic propellants and large initial ullage fractions.

2) The feasibility of improving pressurization performance by causing gas mixing to occur in the ullage has been demonstrated. A reduction of over 50% in the pressurant mass for LH_2 systems is theoretically possible. Significant reductions have been observed experimentally. The straight-pipe injector is effective in causing extensive ullage mixing.

3) The analysis of jet penetration depth and ullage partial mixing agrees well with the available experimental data for straight-pipe injectors.

4) Further study of ullage mixing should include an investigation of gas-liquid interface processes.

References

[1] Roudebush, W. H., "An Analysis of the Problem of Tank Pressurization during Outflow," TN D-2585, Jan. 1965, NASA.

[2] Epstein, M., Georgius, H. K., and Anderson, R. R., "A Generalized Propellant Tank Pressurization Analysis," *International Advances in Cryogenic Engineering*, Plenum Press, New York, 1965, pp. 290–302.

[3] Kendle, D. W., "A Tank Pressurization Computer Program for Research Applications," DAC-63076, Dec. 1968, McDonnell Douglas Astronautics Co.—West, Huntington Beach, Calif.

[4] Nein, M. E. and Thompson, J. F., "Experimental and Analytical Studies of Cryogenic Propellant Tank Pressurant Requirements," TN D-3177, Feb. 1966, NASA.

[5] Kendle, D. W., "Ullage Mixing Effects on Cryogenic Tank Pressurization," DAC-63168, June 1969, McDonnell Douglas Astronautics Co.—West, Huntington Beach, Calif.

[6] DeWitt, R. L., Stochl, R. J., and Johnson, W. R., "Experimental Evaluation of Pressurant Gas Injectors during the Pressurized Discharge of Liquid Hydrogen," TN D-3458, June 1966, NASA.

[7] Laufer, J., "Turbulent Shear Flows of Variable Density," *AIAA Journal*, Vol. 7, No. 4, April 1969, pp. 706–713.

Quenching of Solid-Propellant Rockets by Water Injection

Leon D. Strand* and Walter Gerber†

Jet Propulsion Laboratory, Pasadena, Calif.

Introduction

In other programs, command termination of solid-propellant motors by water quench has been demonstrated in motors having propellant weights up to 8600 kg. However, most attempts to correlate extinguishment data have given questionable results. Three mechanisms have been proposed: 1) rapid cooling of gases causes a dP/dt sufficient for extinction; the water then wets the surface, cooling it to prevent reignition[1]; 2) cooling of the gases below some threshold value lowers heat feedback to the propellant below that necessary for self-supported combustion[2]; and 3) a water film covers the entire surface of the propellant, cooling it below the temperature required for burning.[3,4] The present study was initiated to improve understanding of the quench mechanism and to determine the optimum method of water injection.

The slab-burning window motor used (Figs. 1 and 2) is capable of accepting several different types of water injectors: head-end injectors, multiple injectors impinging normal to the propellant surface, and sheet injectors which lay a thin sheet of water onto the propellant surface. The spray form varied from a fine mist to a solid stream.

High-speed movies were taken during water injection and quenching. To facilitate viewing, a nonaluminized propellant (JPL 540 Mod A) with a polyether-polyurethane binder and ammonium perchlorate oxidizer was used.

Presented as Paper 70-640 at the AIAA 6th Propulsion Joint Specialist Conference, San Diego, Calif., June 15–19, 1970; received June 29, 1970; revision received May 13, 1971. This paper presents the results of one phase of research carried out at the Jet Propulsion Laboratory, California Institute of Technology, under Contract No. NAS 7-100, sponsored by NASA.

* Senior Engineer, Solid Propellant Engineering Section. Associate Member AIAA.

† Senior Test Engineer, Lockheed Aircraft Service Co. (Contractor).

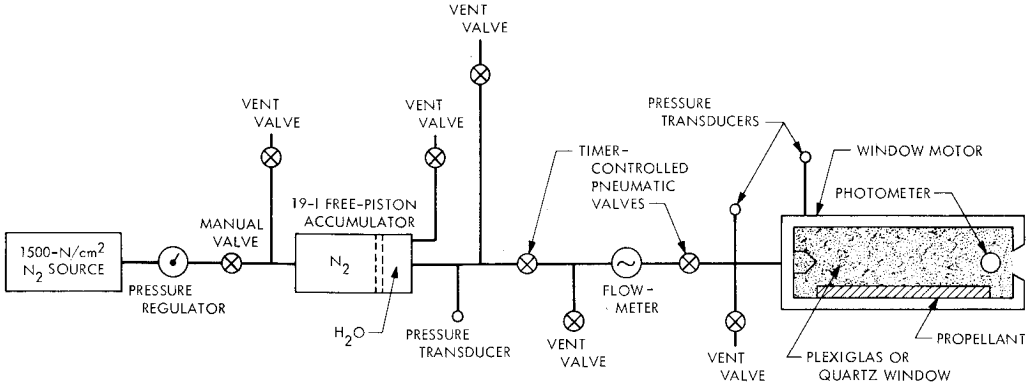

Fig. 1 Schematic diagram of experimental water-quench apparatus.

Test Apparatus

Figure 1 shows the principal components on the main line. The stainless steel motor is 43.7 cm long, 9.52 cm wide, and 11.4 cm high. Slabs of propellant, 34.8 cm long, 4.44 cm wide, and 1.27 cm thick, cast on steel plates, are mounted on either the bottom surface only, or both the top and bottom of the motor. The slabs were restricted on all four sides with a thin layer of vinyl cement that regressed with the burning propellant surface. The nozzle is solid copper and converges to its exit throat diameter d^*, which can be varied from 1 to 2.54 cm.

Figure 2 shows the motor with overhead injectors (Types D-E, Table 1). Only the lower propellant slab was used for this system. The second system, a head-end sheet injector,[5] was designed to lay a thin sheet of water over the lower propellant slab burning surface. The third system was a central head-end injector for flat-jet and atomization type injectors. The motor accepts a Dynisco water-cooled and a Tabor pressure transducer, both of the strain-gage type. Two hot-wire igniters were used in parallel.

Initially, water flow onset was initiated with an explosive valve, but this method proved unsatisfactory, because its opening transient resulted in an initial uncontrollable, high-speed spurt in the water-injection rate. Solenoid-operated valves were used thereafter. In the final setup, two dc Annin valves, one normally open, the other normally closed, were used. Their positions during a test were recorded with linear potentiometers. A turbine-type flowmeter measured the water flow rate.

The Dynisco pressure transducer, Model PT49C-5C(0-345 N/cm²), has a flat (±10%) frequency response[6] to 10,000 Hz. The silicon diode photovoltaic cell used to indicate termination of combustion was mounted facing the motor window; its light sensitivity peaks near 8000 Å. A 16-mm Hycam camera operating at 6000–8000 frames/sec was used for the motion picture coverage. Backlighting of the motor was provided.

The data were amplified and recorded on tape, and played back on an oscillograph.

The test sequence was initiated by closing the hot-wire igniter circuit. When the motor pressure reached 20.7 N/cm², a pressure switch started the camera and the digital timers that actuated the water valve circuit when the camera reached operating speed (1 sec), and nitrogen pressure forced the floating piston to inject water into the motor at the rate and quantity determined by the area of the injectors, the N_2 pressure, and the time interval between actuation of the valves.

A typical test record is shown in Fig. 3. Initiation of the flowmeter signal usually agreed within 2 ms with the valve position and water pressure signals. The volume of water injected Q_ω was obtained by integrating the flowmeter output over the injection time, as indicated by the valve position traces. This was checked beforehand by carefully collecting the injected water and comparing the measured volume with the integrated flowmeter results. Agreement varied from within 90 to 95% for injectant volumes of 5 to 10 ml, to within 70 to 80% for injectant volumes in the 2-to-3-ml range.

Although care was taken to purge the air out of all water lines prior to each test, in motor firings with the overhead injector system, operation of the valves usually resulted in the buildup of pressure oscillations in the water distribution manifold that damped out following closure of the downstream valve. During the latter decay, the flowmeter indicated that 1 to 4 ml of water were injected into the motor. Motion picture coverage in a few tests showed this flow to tail off rapidly to a pulsating dribble.

Table 1 Water injector systems

	Injector	Manufacturer	Diameter, cm
A	Head-end sheet	JPL	0.635
B	Head-end, hollow-cone atomizing	Spraying Systems Co.: ¼ MSS 22 (80°)	0.193
C	Head-end fan spray	Delavan Mfg. Co.: ¾ WF-100-65°	0.635
D	8 solid cone	Delavan Mfg. Co.: ¼ SC-M-10(65°)	0.198
E	8 solid jet	Delavan Mfg. Co.: ¼ WF-8-0°	0.178

Test Results

The five water injector systems that received the most testing are listed in Table 1. The test conditions and the results of each test are listed in Table 2.

Multiple overhead and head-end fan injectors

The test results obtained at a nominal motor chamber pressure P_c of 100 N/cm² (region of specific interest at JPL) are plotted in Fig. 4 as weight of water injected/propellant burning area ratio W_w/A_b vs water injection/propellant gasification rate ratio $\dot{W}_w/\dot{W}_p$. These parameters had been

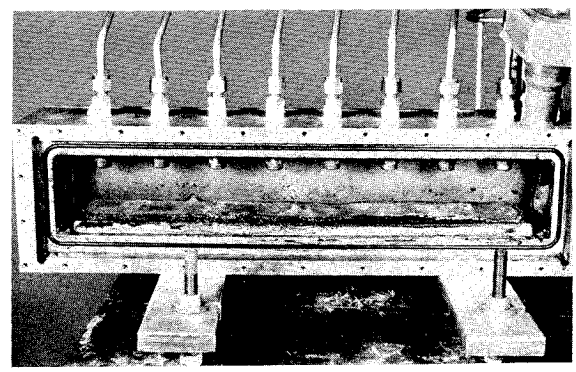

Fig. 2 Post-test view of motor with overhead injector system.

Table 2 Test parameters and results

Injector system	d^*, cm	P_w, N/cm²	P_c, N/cm²	$\dot{W}_w$,[a] kg/sec	$\dot{W}_w/\dot{W}_p$	Q_w, ml	W_w/A_b, kg/cm² × 10^{-5}	$-\dot{P}_{c_i}$, N/cm²-sec
Head-end injectors								
Sheet	1.32	315	103	0.36	4.0	5	2.6	2,200
	1.22	164	110	0.38	4.0	8	4.2	...
	1.22	154	117	0.37	3.9 avg.	17	8.8	...
	1.27	135	89	0.64	7.0 avg.	59	31	1,500
	1.22	383	106	1.32	14.0	40	21	7,200
Atomizing	1.22	1,052	109	0.14	1.3	170	88	3,300
	1.47	672	56	0.10	1.4	60	32	1,700
	1.57	527	43	0.10	1.4	90	47	1,600
Fan	1.83	121	106	0.32	1.6 avg.	20	5.2	1,800
	1.83	172	107	0.74	3.6	19	4.8	5,200
	1.83	192	≈103	0.75	3.7	18	4.5	≈5,500
	1.83	188	95	0.69	3.5	14	3.5	5,700
	1.83	175	96	0.69	3.4	12	3.0	5,300
	1.83	206	≈103	0.70	3.4	9	2.3	≈4,600
	1.83	159	86	0.91	4.7 avg.	77	20	6,700
Normal injectors (8 each)								
Solid cone	1.32	111	100	0.26	2.4 avg.	11	5.2	2,000
	1.32	110	96	0.24	2.2	6.7	3.2	540
	1.32	110	99	0.21	2.0	62	3.0	1,400
	1.32	136	106	0.33	2.9	6	3.0	2,600
	1.32	150	96	0.32	3.0	5	2.4	2,100
	1.32	161	108	0.32	3.0	3	1.4	2,600
	1.27	136	114	0.41	3.4	6	3.0	1,600
	1.12	240	170	0.77	5.8	15.6	7.3	7,400
	1.12	204	162	0.45	3.6	9	4.3	3,800
	1.12	243	171	0.54	4.3	9	4.2	14,500
	1.12	387	173	0.54	4.3	6	2.9	13,000
	1.12	252	151	0.50	4.0	4.2	2.0	3,000
Solid jet	1.32	109	103	0.19	1.8	7.2	3.4	1,400
	1.32	110	98	0.17	1.6	4.3	2.1	1,500
	1.32	112	100	0.15	1.3	3	1.5	1,500
	1.32	112	96	0.20	1.8	3	1.5	...
	1.32	221	105	0.43	4.0	4	1.9	3,100
	1.32	156	100	0.27	2.5	3	1.5	2,300
	1.32	240	99	0.38	3.6	2.5	1.2	830
	1.12	193	159	0.33	2.6	7.2	3.4	1,400
	1.12	226	159	0.31	2.5	5.8	2.8	2,000
	1.12	288	155	0.38	3.1	4	1.9	1,400

found in Ref. 4 to correlate motor test data taken at constant chamber pressure. For $\dot{W}_w/\dot{W}_p$ ratios >3, the small quantities of water required to produce no-quenches approached the accurate measurement limits of the test system. With the overhead solid cone injectors (Fig. 4a), the quench water requirements increased rather sharply with reduction in $\dot{W}_w/\dot{W}_p$. Motion picture data showed that the small water pressure head at the lower injection rates resulted in wispy, underexpanded water jets, and consequently, poor coverage of the propellant surface. At this motor pressure, a reduction in $\dot{W}_w/\dot{W}_p$ did not have a great effect on the minimum injectant quantity required for quench using the overhead solid-jet injectors (Fig. 4b). The single head-end fan injector was aligned vertically, so that the water fan spread over two propellant slabs. All but one of the data points (Fig. 4c) were at a nominal $\dot{W}_w/\dot{W}_p$ value of 3.5. This injector produced the most rapid depressurization of the motor (see Table 2).

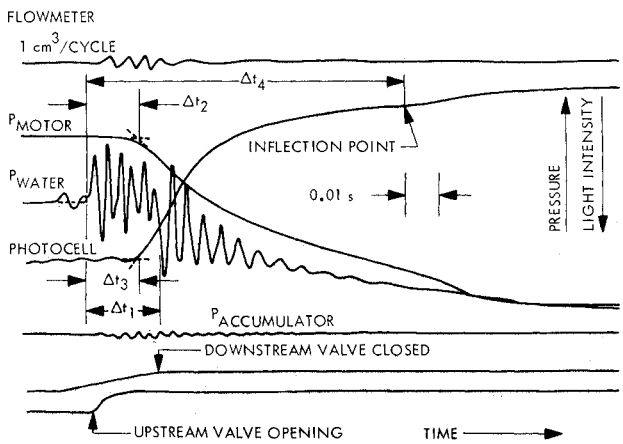

Fig. 3 Typical test record.

Head-end sheet and atomizing injectors

Complete water coverage of the burning propellant surface could not be obtained with the head-end sheet injector. In five tests ($\dot{W}_w/\dot{W}_p$ = 4.0 − 14, W_w/A_b = 0.000026 − 0.00031 kg/cm²) portions of the propellant at the forward end of the motor continued to burn during the water injection.

Three tests (P_c = 110, 55, and 40 N/cm²) were carried out with a head-end atomizing injector to determine whether, by rapidly cooling the gases, a rapid depressurizing quench could be induced. The water spray produced initial depressurization rates $-\dot{P}_{c_i}$ of 3300, 1700, and 1600 N/cm²-sec, respectively. For the 55 and 40 N/cm² tests, these initial depressurization rates were greater than those found sufficient to produce quench in earlier rapid depressurization experiments,[7] but the propellant recovered in both tests and continued to burn.

The 160 N/cm² tests

Several tests were performed at a nominal motor pressure of 160 N/cm²; with the solid-jet and solid-cone overhead

Table 2 continued

Injector system	P_c, N/cm²	Δt_1,[b] ms	Δt_2,[c] ms	Δt_3,[d] ms	Δt_4,[e] ms	Results[f]
Head-end injectors						
Sheet	103	9	6	6	...	*NQ*
	110	22	15	14	...	*NQ*
	117	46	16	17	...	*NQ*
	89	95	17	17	32	*PQ*
	106	32	11	11	16	*PQ*
Atomizing	109	1,500	3	5	5	*PQ*
	56	570	3	7	...	*NQ*
	43	900	2	5	...	*NQ*
Fan	106	66	20	28	40	*Q*
	107	19	12	15	26.5	*Q*, reignited
	≈103	23	9	9	19	*Q*
	95	19	10	11	16	*Q*
	96	19	11	14	29	*Q*
	≈103	12	11	13	...	*NQ*
	86	80	13	15	20	*Q*, rapid
Normal injectors (8 each)						
Solid cone	100	41	26	26	85	*Q*
	96	23	24	35	...	*NQ*
	99	23	24	23	...	*NQ*
	106	15	15	17	85	*Q*, reignited
	96	12	15	15	70	*Q*, reignited
	108	9	12	18	...	*NQ*
	114	30	15	15	36	*Q*, reignited
	170	27	11	13	17	*Q*, rapid
	162	21	16	17	24	*Q*
	171	16	10	11	16	*Q*, reignited
	173	10	7	8	14	*Q*, rapid
	151	9	11	12	...	*NQ*
Solid jet	103	34	18	18	90	*Q*, very slow
	98	20	13	14	104	*Q*, very slow
	100	11	16	16	148	*Q*, very slow
	96	10	14	...	...	*NQ*
	105	9	9	9	16	*Q*, slow
	100	9	10	No data	No data	*Q*
	99	9	9	No data	...	*NQ*
	159	21	16	16	...	*NQ*
	159	10	10	15	...	*NQ*
	155	4	8	6	...	*NQ*

[a] Representative measured flow rate, except where noted.
[b] Injection time interval, as indicated by valve position and water pressure head signals (Fig. 3).
[c] Time from initiation of water injection to initial drop in motor pressure (Fig. 3).
[d] Time from initiation of water injection to initial drop in photocell signal (Fig. 3).
[e] Time from initiation of water injection to point of inflection in photocell signal (Fig. 3).
[f] *Q* = quench; *PQ* = partial quench; *NQ* = no quench.

injector systems at $\dot{W}_w/\dot{W}_p$ ratios of 2.5 to 3 and 4, respectively. In accordance with the findings of previous investigators,[3,4] the water quantities required for quench increased with increasing pressure. Because at a motor pressure of 100 N/cm² the solid-jet injector quench requirements were rather insensitive to $\dot{W}_w/\dot{W}_p$, it was felt that they might also show a smaller motor pressure effect. This, however, was not the case, as no quenches were obtained in the three tests conducted.

Time to quench

In a majority of the quench tests, the photocell output signal began to decrease irregularly at some time after the onset of water injection until a point of inflection occurred, following which the signal decreased steadily in output to the ambient level (Fig. 3). Because of its behavior with changing pressure venting rate in an earlier rapid depressurization quench study,[7] the time Δt_4 to this inflection point had been assumed to be the time of quench. The Δt_4 are plotted vs $\dot{W}_w/\dot{W}_p$ for the overhead solid-cone, overhead solid-jet, and head-end fan spray injector systems tests in Figs. 5a, 5b, and 5c, respectively. For the overhead injectors, the quench times appear to level off for $\dot{W}_w/\dot{W}_p \geq 5$. The times increased rapidly with decreasing $\dot{W}_w/\dot{W}_p$ for both injectors. Scattering occurred in the data for the head-end fan spray injector, and only one low $\dot{W}_w/\dot{W}_p$ point was obtained, but the time delay appears to be less sensitive to the $\dot{W}_w/\dot{W}_p$ ratio for this injector system.

Motion picture data

For the overhead injectors, water transient time for the 2.8 cm travel from the injectors to the propellant surface was 1 to 3 msec. The over-all quench process was slower at the higher motor pressure. In general, the propellant surface region would begin to darken 10 to 20 msec after the initiation

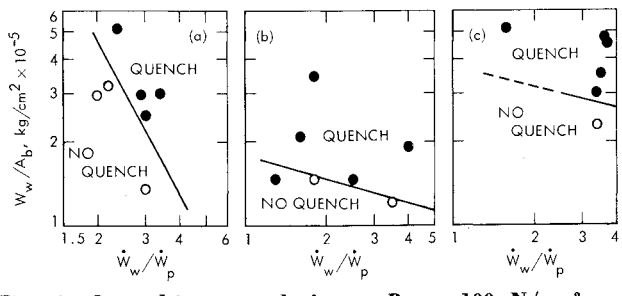

Fig. 4 Quenching correlations; $P_c \simeq 100$ N/cm²: a) overhead, solid-cone injectors; b) overhead, solid-jet injectors; and c) head-end fan spray injector.

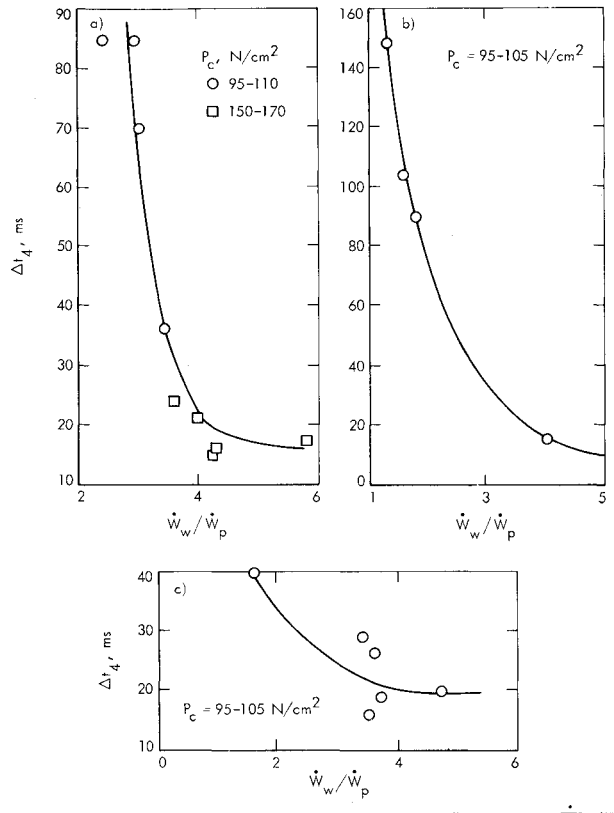

Fig. 5 Photocell inflection-point time delay Δt_4 vs $\dot{W}_w/\dot{W}_p$ for three injector types: a) overhead, solid-cone injectors; b) overhead, solid-jet injectors; and c) head-end fan spray injector.

of water flow and, for no-quenches, begin to recover 10 to 60 ms later, depending on how marginal the test was. Once initiated, quenching, as indicated by darkening of the combustion zone, took place in milliseconds. With the solid-jet injectors, darkening of the burning surface first occurred in the impingement area and then propagated outward.

On a few of the quench tests, quenching of the restricted edge was quite delayed. Also, in marginal no-quench tests, the restricter material continued to decompose and smoke, indicating that it retained its thermal energy or that some burning activity may have persisted at the propellant-restricter interface.

Summary of Results and Conclusions

Tests at P_c = 100 N/cm² indicated that 1) For water injection normal to the propellant surface, with a decrease in $\dot{W}_w/\dot{W}_p$, a) minimum water requirements for quench increased slightly for solid-jet and showed a marked increase with solid-cone injectors, and b) quench times increased rapidly for both systems. 2) At the low $\dot{W}_w/\dot{W}_p$ conditions, drag effects on the solid jet were probably still small in this small motor, while the solid-cone plume expansion became insufficient for good water coverage of the propellant surface, providing probable explanations for 1a above. 3) Because of the more efficient water distribution of the overhead systems, minimum water requirements were lower than those of the head-end fan spray injector at the baseline $\dot{W}_w/\dot{W}_p$ test conditions (3 to 4). 4) The measured minimum water quantities agree quite well with the results of laboratory tests[3] conducted in the same pressure range. 5) Marginal or no-quench usually occurred when the water injection time Δt_1 was less than the times from initiation of water injection to the initial drop in motor pressure Δt_2 and photocell output Δt_3. Water quantities required for quench increased with increased pressure.

Attempts to obtain a dP_c/dt quench by rapidly cooling the motor gases with an atomization injector were not successful, although only a few tests were made. Difficulties encountered in quenching at propellant-restricter interfaces could be an important consideration in the design of motors utilizing thrust termination by water injection. Similarly to the findings of Ref. 3, it is concluded that for rapid, positive quenches, $\dot{W}_w/\dot{W}_p$ should not be less than 4 to 5.

It is concluded, from the motion picture data, that thermal quenching of the propellant burning surface and continued cooling of the surface until the hot gases have been exhausted provide a reasonable model for describing the propellant extinguishment characteristics.

References

[1] Taback, H. J., Day, E. E., and Browne, T. P., "Combustion Termination of Solid Rocket Motors," *Journal of Spacecraft and Rockets*, Vol. 2, No. 3, May-June 1965, pp. 332–337.

[2] Jaroudi, R. and McDonald, A. J., "Injection Thrust Termination and Modulation in Solid Rockets," *AIAA Journal*, Vol. 2, No. 11, Nov. 1964, pp. 2036–2038.

[3] "Demonstration of a Solid Propellant Motor Malfunction-Detection and Combustion Termination System, Vol. 1—Phase 1, Combustion Termination," Final Rept. NASA 8-20219, June 1967, Aerojet-General Corporation, Sacramento, Calif.

[4] Nielsen, F. B., "Combustion Termination System for 120-inch-Diameter Solid Rocket Motor (Titan III-C)," Rept. AFRPL-TR-66-260, Oct. 1966, United Technology Center, Sunnyvale, Calif.

[5] Riebling, R. W., "The Formation and Properties of Liquid Sheets Suitable for Use in Rocket Engine Injectors," TR 32-1112, June 1967, Jet Propulsion Lab., Pasadena, Calif.

[6] Thomas, J. P., "Summary Technical Report on Transient Pressure Measuring Methods Research," Aeronautical Engineering Rept. 595p. Nov. 1965, Princeton Univ., Princeton, N.J.

[7] Gerber, W., "Experimental Study of the Combustion Termination of a Solid Propellant by Rapid Depressurization," Space Programs Summary 37-61, Vol. III, Supporting Research and Advanced Development, Feb. 1970, Jet Propulsion Lab., Pasadena, Calif., pp. 200–206.

Full-Scale Flight Test Base Pressure Results for a Blunt Planetary Entry Probe Configuration

J. M. Cassanto*
General Electric Company, Philadelphia, Pa.

Introduction

BASE pressure measurements from a planetary entry probe can provide a direct method of deriving the freestream static pressure profile (P_∞) of a planet.[1] However, base pressure data for planetary entry type configurations are limited to the ground test data of Refs. 2–7, and full-scale NASA Ames flight data from Refs. 8 and 9. The purpose of this Note is to present additional, hitherto unpublished, full-scale flight test base pressure data from several flights of a blunt

Received March 11, 1971; revision received May 12, 1971. The present flight test data results are a re-evaluation of flight test data that were originally reduced and analyzed by D. Griffith of General Electric in 1959. The author gratefully acknowledges the assistance of Griffith in preparing the present note and the assistance of C. Dudzinski who reduced and plotted the present flight results.

Index category: Spacecraft Flight Testing; Jets, Wakes, and Viscid-Inviscid Flow Interactions; Entry Vehicles and Landers.

* Consulting Engineer, Aerodynamics Laboratory, Re-entry and Environmental Systems Products Division. Member AIAA.